COMPRESSIVE BEHAVIOR OF PERLITE/SODIUM SILICATE COMPOSITE FOAM MODIFIED BY BORIC ACID

Pranto Karua, Md. Arifuzzaman *

Department of Mechanical Engineering, Khulna University of Engineering & Technology, Khulna 9203, Bangladesh

Abstract

In this work lightweight expanded perlite/sodium silicate composite foams were manufactured with varying quantities of boric acid (BA) 0-2.88 wt.%. The composites were characterized for density, compressive strength (CS), compressive modulus (CM), and energy absorption (EA) up to 50% strain. The compression tests were also conducted at various crosshead speeds to evaluate the strain rate dependency of the foams. The hygroscopic tests were done to evaluate water absorption properties and investigate the effects of water absorption on the compressive properties of the foams. The CS, CM, and EA of the foams increased for a boric acid content of 0.74 wt.%, but further addition of BA caused a gradual decrease in these characteristics. The range of sp. CS (3.80-5.93 MPa/(g/cm^3)) achieved were found to be well compatible with the values of building materials in the literature. The foams appeared to be sensitive to the strain rate in compression, causing variations in the compressive properties as well as the trends of stress-strain curves. Furthermore, the addition of BA in the composite reduced water absorption up to a BA content of 1.46 wt.%. The compressive properties were also highly influenced by the hygrometric test.

Keywords: lightweight perlite composite; sodium silicate solution; boric acid; compressive behavior; strain rate sensitivity; hygroscopic test.

Introduction

With the increasing concern on building energy consumption, the use of inorganic insulating materials is getting attention day by day which leads to the development of new building materials. The pioneers in this sector are looking forward to introducing lightweight materials instead of wood or concrete to minimize the costs as well as energy consumption. This purpose has already come into consideration by using

*Corresponding author: Md. Arifuzzaman, *arif48@me.kuet.ac.bd*

composites/foams of different lightweight materials. Expanded perlite-based lightweight materials offer excellent heat and sound insulation. Expanded perlite is broadly used in the construction, industrial, chemical, horticultural, and petrochemical industries [1]. Perlite is mainly available in its expanded form and possesses outstanding thermal insulation and fire-resisting properties [2]. Different materials are combined with perlite to improve the properties of the resulting composites.

Rashad reviewed expanded perlite-based building materials and the advantages of using expanded perlite as a building material such as lessening CO_2 emission into the atmosphere, reducing consumption of limestone and sand by the cement industries. In addition, he also discussed expanded perlite-based materials fire-resisting, sound insulation, water absorption, and thermal diffusive properties [1]. *Zhang et al.* used hydrophobic expanded perlite as an external wall insulation material to serve the purpose of reducing the rate of water absorption and also to resist the freeze-thaw problem in cold areas [3].

Sengul et al. investigated the effect of expanded perlite on lightweight concrete keeping water to cement ratio constant and noticed a reduction in thermal conductivity of the mixtures as compared to the raw concrete. They concluded that the compressive strength and modulus of elasticity of concretes decreased with the increasing content of expanded perlite [4]. *Pramusanto et al.* proposed a high-strength lightweight concrete using expanded perlite as the lightweight aggregate and recommended 50% expanded perlite, 50% natural sand, and the aggregate composition of 80% with the cement as an optimum mixing percentage [5].

Celik et al. conducted experiments on composites made of perlite, pumice, and cement to improve thermal resistance, and noticed a significant decrease in thermal resistance with the increase of moisture [6]. *Ye et al.* added a liquid hydrocarbon named RT28 with cement/expanded perlite composite and found a linear increase in compression strength with increasing the mass fraction of RT28, however, the thermal conductivity of the composite increased as well [7].

Bozkurt et al. researched a perlite aggregate mixed with flax fibers and polypropylene fibers to improve the sound absorption properties of the plaster layer and noticed a positive impact of adding a lightweight perlite aggregate. Furthermore, they also discovered that how the effectiveness of flax fiber in improving sound absorption properties at both high and low frequencies, whereas polypropylene fiber was only effective at absorbing high frequencies [8]. *Yanjun et al.* used the vibration molding method to construct a perlite board and concluded that the perlite board formed by vibration molding showed a more uniform density and a better effect on sound absorption only if the vibration are maintained within the frequency range of 28 Hz to 32 Hz [9].

Yao et al. found a method of reducing inner room temperature by incorporating PCMW, made of expanded perlite and paraffin, in the inner walls, together whit a delayed peak temperature timing. According to their numerical study, a typical office building having a 4000 m^2 area incorporated with PCMW can reduce the inner temperature by almost 9.22 K [10]. *Sun et al.* investigated the effect of paraffin/expanded perlite materials on cement mortar and showed that cement mortar with 20 wt% paraffin/expanded perlite materials has a good heat storage capacity. However, with the increasing amount of paraffin/expanded perlite materials compressive strength and flexural strength of cement mortar decreased [11].

Jia et al. developed a novel aerogel/expanded perlite (AEP) based composites to reduce its water absorption. They also found improvements in thermal conductivity and durability [12]. *Wu et al.* fabricated an expanded perlite-coal fly ash/aluminum dihydrogen phosphate-water-based insulation board following a mass ratio of 1:19:6:14–4:16:6:14. The prepared composite showed bulk densities from 253 kg m^{-3}– 305 kg m^{-3}, compressive strengths 0.428 MPa–0.462 MPa, and the heat conductivities 0.073 Wm^{-1}K^{-1}–0.082 Wm^{-1}K^{-1} [13].

Fu et al. [14] introduced a vacuum impregnation method to prepare $CaCl_2 \cdot 6H_2O$/Expanded perlite composite, showing larger apparent specific heat as compared to the polystyrene foam but the composite exhibited a rise in indoor temperature having higher thermal conductivity. *Alam et al.* fabricated composites included with 30% expanded perlite, 50% fumed silica, SiC, and polyester fibers to replace pure fumed silica-based vacuum insulation panels (VIP) considering the cost-effectiveness. In addition, they also quantified the opacifying properties and the radiative conductivity [15].

Gao et al. designed triple-hierarchical porous structures by combining the ambient temperature foam method and simple heat treatment on expanded perlite/ cetyltrimethyl ammonium bromide, H_2O_2 based composites. They reported a reduction in thermal conductivity and density by approximately 10% and 15% respectively, while also noting an 80% improvement in the softening coefficient of the composites [16]. *Lin et al.* invented the expanded perlite (EP)/wood-magnesium (EPWMC) composite. They observed that EPWMC composites filled with 60–70 mesh EP had a thermal conductivity of 0.0869 Wm^{-1}K^{-1} and exhibited excellent flame retardant and smoke suppression performances [17].

Skubic et al. developed a mathematical model to predict the sintering temperature of expanded perlite/sodium silicate composite and determined that the sintering temperature increased with decreasing the sodium silicate contents [18]. *M. Arifuzzaman et al.* characterized expanded perlite/sodium silicate-based composites and achieved 1 MPa compressive strength at a density of 0.3 g/cm^3 without any reinforcement. They also analyzed the prepared composites based on particle size, compaction pressure, compressive strength, and volume fraction of the constituents [19].

Adhikary et al. showed the improvement in compressive properties of expanded perlite/sodium silicate composites with the reinforcement of corn starch [20], while *Tian et al.* showed the effect of sodium silicate on expanded perlite and discovered a gradual increase in apparent density, tensile strength, flexural strength with the increase in sodium silicate contents on perlite [21].

Uluer et al. applied five different models to investigate the thermal conductivity performance of expanded perlite mixed with sodium silicate, NaOH, and H_2O_2. They suggested that the panel prepared with 94-96% E.P and 4-6% binder by volume had the lowest thermal conductivity [22]. *Gao et al.* formed perlite/sodium silicate, H_2O_2, cetyltrimethyl ammonium bromide, and rock-wool based non-inflammable insulating materials which showed improved mechanical strength (0.09–0.6 MPa) with low thermal conductivities (0.040–0.060 Wm^{-1}K^{-1}) [23].

Zhang et al. prepared capric acid–palmitic acid/EP composite PCM based on gypsum as an energy storage material. They monitored the increment in energy storage capacity with the increasing volume content of PCM on gypsum but the bending strength and compressive strength of the PCM gypsum board were decreased by 56% and 40.4% respectively as compared to the pure gypsum board [24]. Many researchers have worked on the development of expanded perlite-based composites as described earlier. However, there is scope for improvement and exploration for novel behavior of the expanded perlite-based composites.

Recently, *Li et. al.* developed an adiabatic foam using sodium silicate solution with boric acid. They found a significant improvement in compressive strength with the addition of boric acid in the sodium silicate solution [25]. The expanded perlite/sodium silicate composite reported by *Arifuzzaman et al.* may further be improved with the addition of boric acid in the sodium silicate solution [19].

Besides, the hygroscopic properties and strain rate sensitivity of expanded perlite/sodium silicate composite foams also need exploration to completely understand their behavior. These properties of expanded perlite/sodium silicate composites foam have never been studied to the best of the authors' knowledge.

In this work, boric acid was used as a reinforcement to sodium silicate solution for the development of a novel lightweight composite foam to be used as a core of sandwich structures for both building and marine structures. The effects of boric acid content, loading rate, and water absorption on the compressive properties of the foam are presented.

Materials

Expanded Perlite

Expanded perlite was bought from Xinyang Caster New Material Co. Ltd., Henan Province, China. The particles of sizes 2-3 mm were separated using sieves to maintain homogeneity. The powders and the particles of less than 2 mm and greater than 3 mm were screened out. According to the manufacturer's catalog, the expanded perlite contains 71-75% silicon oxide, 12-16% aluminum oxide, 2.5-5% sodium oxide, 1-4% potassium oxide, 0.1-2% calcium oxide, 0.15-1.5% ferric oxide and 0.2-0.5% magnesium oxide. The bulk density was measured from the mass of the particles covering 400 cm^3 of a cylinder volume which is 0.071 g/cm^3.

Mix Design

Sodium silicate solution (SSS) has been collected from Silica Solution, Chittagong, Bangladesh to be used as the binder. According to the manufacturer's datasheet, the weight ratio of SiO_2 and Na_2O is 3.2:1 with a density of 1.381 g/cm^3 at 20 °C and the solid content of sodium silicate of 36.3 ± 1.2% (by weight). Boric acid and gypsum powder were purchased from the local construction shops in powder form to be used as reinforcement to the sodium silicate solution. For the mix design, the mass of perlite and gypsum were kept constant while the mass of boric acid was varied from 0 to 8 g as shown in Table 1.

Table 1. Mixing proportions of the constituent materials.

Sample No.	Mass of perlite (g)	Mass of SSS (g)	Mass of gypsum (g)	Mass of boric acid (g)	Percentage of boric acid, wt.%
1.	50	200	20	0	0
2.	50	200	20	2	0.74
3.	50	200	20	4	1.46
4.	50	200	20	6	2.17
5.	50	200	20	8	2.88

Methodology

Sample preparation

Perlite foams were manufactured by mixing expanded perlite particles of 2-3 mm size with sodium silicate solution (SSS), gypsum, and boric acid according to the mix proportion given in Table 1. The mixing was done part by part, firstly the gypsum powder was poured into the SSS solution and the mixture has been hand-stirred at a moderate speed using a mild steel rod for 5 minutes followed by the addition of boric acid with a 5 min stirring in the same manner. The mixture was then poured into a container with perlite particles and hand-mixed to ensure the wetting of all perlite particles. The wet mixture was poured into an aluminum mold of cavity size 130 mm × 130 mm × 25 mm for compression molding. A cover plate was used to compact the wet mix on the mold cavity to 20 mm height. The compacted wet mix was kept inside the Gallenkamp OHG097 XX.2.5 Size 2 oven at a temperature of 120 °C for 4 hours. After that, the cover plate was removed from the top and again kept for drying inside the oven for another 4 hours followed by the removal of the side plates of the mold. The foam panel was kept inside the oven for another 16 hours for final curing. For each boric acid content, two foam panels were made for various tests, and the specimens were taken from both panels for each test. For density, compressive and hygrometric tests the panels were cut into the size of 25 mm × 25 mm × 20 mm, and for flexural tests, the specimen size was 130 mm × 25 mm × 20 mm.

Test Methods

Density Test

Four specimens for each percentage of boric acid content were taken to measure the density. The dimensions (i.e. length, width, height) were measured using slide calipers (Mitutoyo 500-712-20; 0-150 mm) and the mass of all the specimens was measured using a weighing scale (A & D EK-600i; 0.01-600 g). The density was found from the ratio of the mass of the specimen to the volume of the specimen.

Compression Test

   The compression tests were performed on the universal testing machine (Shimadzu AGX 300 kN) by following ASTM C365/C365M standard at a crosshead speed of 5 mm/min. The compression platens were lubricated using gear oil (Fuchs Gear Oil Grade-90) to minimize friction. The compressive strength, compressive modulus, and energy absorption were calculated using ASTM C365/C365M standard from the test results of four samples for each SSS/boric acid ratio. The failure behavior during compression tests was recorded using a video camera for further analysis. The compression tests were also carried out at crosshead speeds of 100 mm/min and 400 mm/min to observe the strain rate sensitivity of the manufactured composites.

Hygroscopic Test

   Six specimens were taken for each SSS/boric acid ratio for the hygroscopic test according to ASTM D5229/D5229M standard. The dimensions and mass of all specimens were measured before immersing them in the distilled water. The specimens were immersed for 48 hours and the dimension and mass were recorded every two hours. The percentage increase in mass and water uptake per unit volume after 24 hours and 48 hours were calculated.

Compression after Hygroscopic Test

   After the completion of the hygrometric test, the wet specimens were kept at atmospheric temperature for 12 hours. The wet specimens were taken to perform compression tests on the universal testing machine (UTM) by following ASTM C365/C365M standard at a crosshead speed of 5 mm/min. The compressive strength, compressive modulus, and energy absorption were calculated using ASTM C365/C365M from the test results of three specimens for each SSS/boric acid ratio. Another batch of specimens are dried in the oven for 24 hours and then the compression test was conducted to measure the compressive properties after drying for comparison with the freshly manufactured specimens.

Results and Discussion

Physical Properties

   The average densities of the composite foams are plotted as a function of boric acid content in the foam in Fig. 1. As expected the density increased linearly with increasing boric acid content in samples. After regression analysis, a linear least square line of y = 0.0066x + 0.4109 and a high Pearson's correlation coefficient of 0.8455 are found indicating high linearity. The minimum density is observed for the sample without any boric acid which is 0.407 g/cm^3 and after the gradual increase with increasing boric acid content, the maximum density is found to be 0.427 g/cm^3 for the maximum boric acid content of 2.88 wt.%. The percentage increase in density based on the control sample (without boric acid) is 4.91% which is not as significant as indicated by the standard deviations (shown as error bars in Fig. 1).
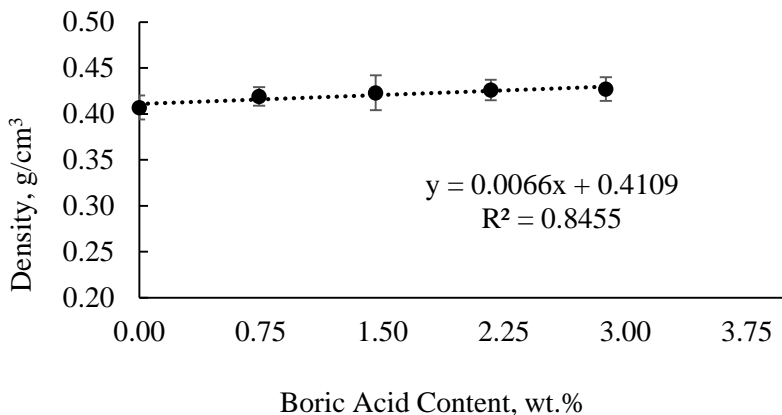
$y = 0.0066x + 0.4109$
$R^2 = 0.8455$

Fig. 1. The density of composites for various weight contents (the standard deviations from four samples are shown as error bars).

Compressive Properties

The compressive strength (CS) and specific compressive strength for various boric acid contents in the composites are shown in Fig. 2. The CS and the sp. CS increased by approximately 5.51% and 2.42% respectively with the addition of 0.74 wt.% boric acid in the composite. The highest CS and sp. CS were 2.49 MPa and 5.93 MPa/(g/cm^3) respectively which are both for the composite with 0.74 wt.% boric acid. The further addition of boric acid in the foam resulted in an abrupt decrease in both the CS and sp. CS as shown in Fig. 2. The maximum decrease in CS and sp. CS (i.e. 31.36% and 34.37% respectively) is seen for the specimen with 2.88 wt.% boric acid.
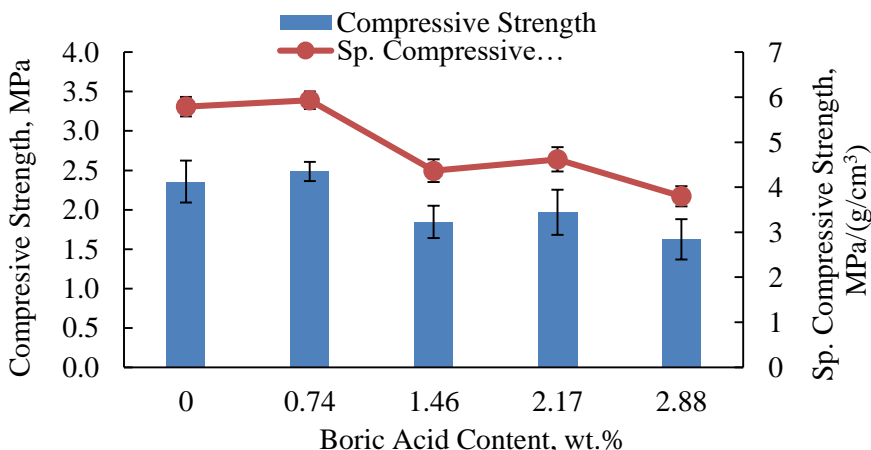
Fig. 2. Compressive strength and specific compressive strength of composites for various boric acid contents
(Standard deviations from four samples are shown as error bars).
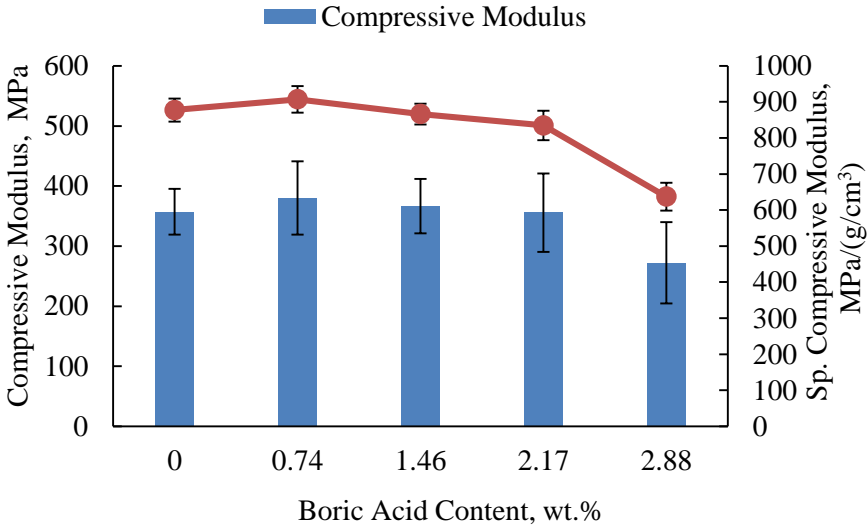
*Fig. 3. Compressive modulus and specific compressive modulus of composites for
various boric acid contents
(Standard deviations from four samples are shown as error bars).*

The compressive modulus (CM) and the specific compressive modulus are plotted for various boric acid contents in Fig. 3. The maximum CM and sp. CM were found for the composite with 0.74 wt.% boric acid (i.e. 380.06 MPa and 907.07 MPa/(g/cm^3) respectively) and the minimum CM and sp. CM (i.e. 272.05 MPa and 637.12 MPa/(g/cm^3) respectively) were found for the composite with 2.88 wt.% boric acid. The observation is analogous to the CS and sp. CS as described in the earlier paragraph. The percentage increase in CM and sp. CM for composite with 0.74 wt.% boric acid from the control sample with no Boric Acid is 6.43% and 3.38% respectively. However, the CM and sp. CM decreased gradually as shown in Fig. 3 with the increased boric acid content to 1.46 wt.%, 2.17 wt.%, and 2.88 wt.%, unlike the abrupt drop in CS and sp. CS as seen in Fig. 2.

The reason for the drop in the compressive properties may be explained as follows. During manufacturing, after the addition of boric acid in the sodium silicate solution, some agglomeration was noticed. The agglomeration was seen to become significant with the addition of a larger amount of boric acid (e.g. 1.46-2.88 wt.%) in SSS while it was not substantial for low boric acid addition (e.g. 0.74 wt.%). The addition of boric acid to sodium silicate was made following the mix proportion described by *Li et al.* who showed the effect of boric acid content (1 – 4 wt.%) on sodium silicate based on density, thermal conductivity, and compressive strength [24]. Because of increasing the viscosity, all the properties increased up to 3 wt.% boric acid, but it started to decrease with more than 3 wt.% boric acid as they concluded [24]. *Li et al.* found that the addition of boric acid in the sodium silicate solution caused an increase in compressive strength in their adiabatic foam up to 3 wt.% boric acid in SSS [25]. However, in their case, the agglomeration did not have a significant effect because their specimens did not have any other load-bearing element. In this research expanded perlite, which is a load-bearing element, has a considerable contribution to the failure behavior of the composite. Because of the

formation of agglomerate the binder could not be distributed properly to hold the expanded perlite particles together. Hence the compressive properties appeared to be decreased in specimens with more than 0.74 wt.% boric acid.

A comparison of CS and sp. CS of the similar lightweight building materials from literature is presented in Table 2. *Shastri and Kim* reported the expanded perlite/potato starch composites with a range of CS 0.1-1.45 MPa and the density range (0.1-0.4 g/cm^3) [26]. *Colak* investigated the effect of foaming agents on the compressive properties of foamed gypsum and showed the CS and sp. CS ranges of 0.35-2.22 MPa and 0.62-2.03 MPa/(g/cm^3) respectively [27]. *Arifuzzaman and Kim* reported CS and sp. CS ranges of 0.20-2.80 MPa and 0.8-5.37 MPa/(g/cm^3) respectively for expanded perlite-sodium silicate composites [19], while *Vimmrova* found the sp. CS within the range 1-3.86 MPa/(g/cm^3) for the gypsum foams of density 0.28-0.55 g/cm^3 [28]. *Adhikary et al.* manufactured expanded perlite-sodium silicate composites reinforced with corn starch and showed the sp. CS in the range of 4.27-5.08 MPa/(g/cm^3) [20]. *Allameh-Haery et al.* investigated the effect of density on expanded perlite–epoxy composites and shown an sp. CS range of 1.10-3.70 MPa/(g/cm^3) [29]. The composites reported in this study displayed the sp. CS range of 3.80-5.93 MPa/(g/cm^3) which are well-compatible with the lightweight building boards in terms of their strength and lightweight when compared with the literature.

Table 2. Comparison of compressive strength and specific compressive strength.

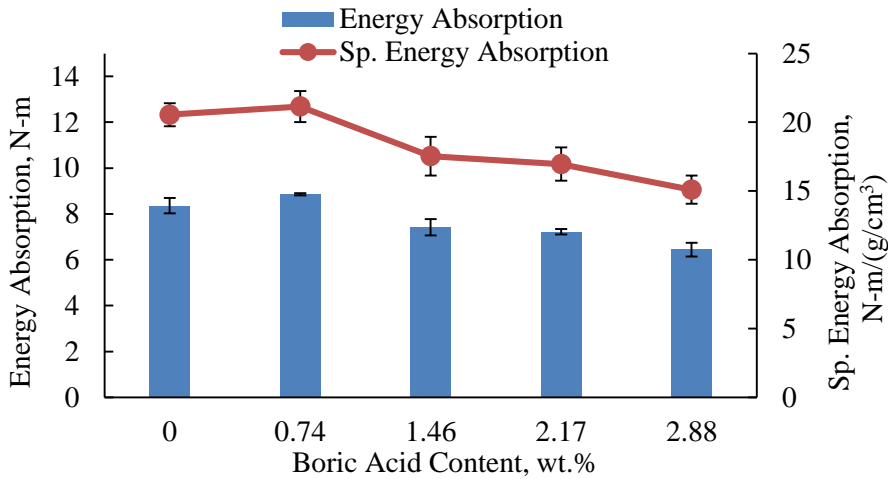| References	Density, g/cm^3	Compressive strength, MPa	Sp. com. strength, MPa/(g/cm^3)
Shastri and Kim [26]	0.1-0.4	0.1-1.45	1-3.63
Colak [27]	0.75-1.08	0.35-2.22	0.62-2.03
Arifuzzaman and Kim [19]	0.2-0.5	0.20-2.80	0.8-5.37
Vimmrova et al. [28]	0.28-.55	0.3-2.7	1-3.86
Adhikary et al. [20]	0.45-0.64	1.93-3.25	4.27-5.08
Allameh-Haery et al. [29]	0.17-0.44	0.17-1.63	1.10-3.70
Current study	0.41-0.43	1.62-2.49	3.80-5.93

Fig. 4. The energy absorption and specific energy absorption during compression up to 50% deformation of composites for various boric acid contents (Standard deviations from four samples are shown as error bars).

In Fig. 4, the energy absorption (EA) and specific energy absorption during compression up to 50% deformation for various boric acid content are plotted from the results of the compression tests. The composite foam with 0.74 wt.% boric acid showed the highest EA and sp. EA and the percent rise compared to the control sample are 5.96% and 2.93% respectively. Further addition of boric acid in the foam resulted in a gradual decrease in both the EA and sp. EA as seen in Fig. 4. The decrease in energy absorption during compression is also related to the compressive properties of the composite and the reason for such behavior is already discussed earlier.

Stress-Strain Curves and Failure Analysis

Typical stress-strain curves of the composites for various boric acid contents are plotted in Fig 5 (a). All curves show a similar trend. The stress increases linearly with strain until a preliminary yielding is noticed at approximately 0.3 MPa followed by a small plateau as shown by the circle in Fig. 5 (b). The reason for this small plateau is the irregular surface of the specimens due to expanded perlite particles. Typical photographs of the surface of the composite are given for clear understanding in Fig. 5 (c). The proper contact is established after this initial plateau after the breakage of the surface particle bumps. Further loading showed a linear increase in stress again up to a maximum then the failure is represented by the gradual drop in stress. In some cases, a second peak after failure is also noticed however the value of the second peak stress is below the first peak stress. One of the important features of the stress-strain curves is their long plateau region indicating the high energy absorption capability of the composites.
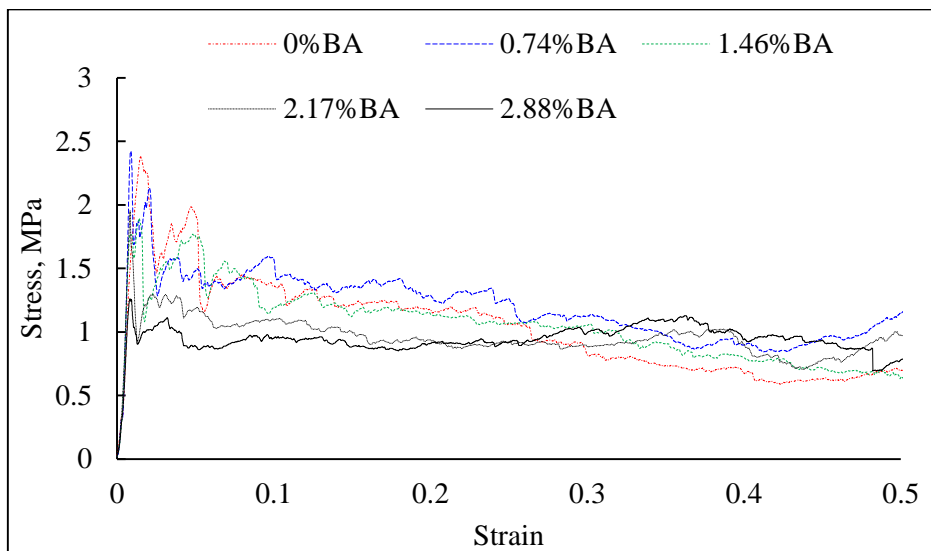
(a)
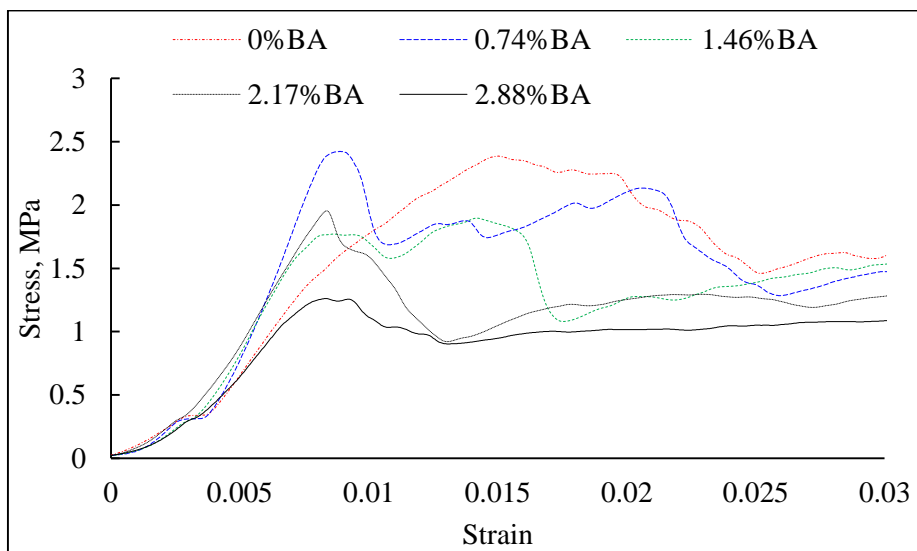
(b)
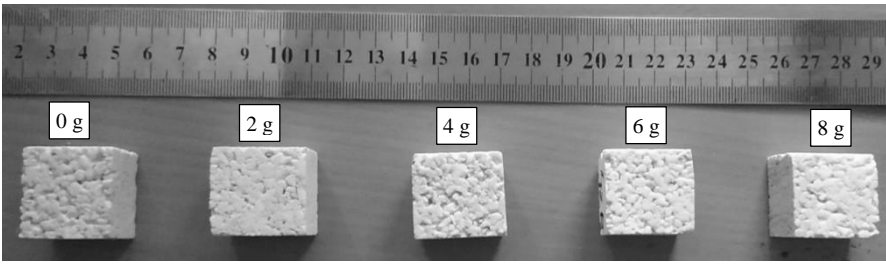
(c)

Fig. 5. (a) Some typical stress-strain curves of the specimens for various wt% of boric acid contents; (b) magnified curves in Fig. 5 (a), and (c) photographs of the uneven surface of the specimens.

To demonstrate the failure mechanism a typical stress-strain curve (for a specimen of 0.74 wt.% boric acid) along with pictures taken during compression test at various strains is given in Fig. 6. It is physically observed that when the stress reached the peak (Point 0), no crack was visible to the naked eye. However, after the peak at Point 1, multiple cracks with no definite orientation were visible as shown in Fig. 6 (b) photograph no. 1 indicating a multiple cracking/sliding planes failure mode which was also observed by *Shastri and Kim* [26]. The failure mode became clearer as the compression propagated.
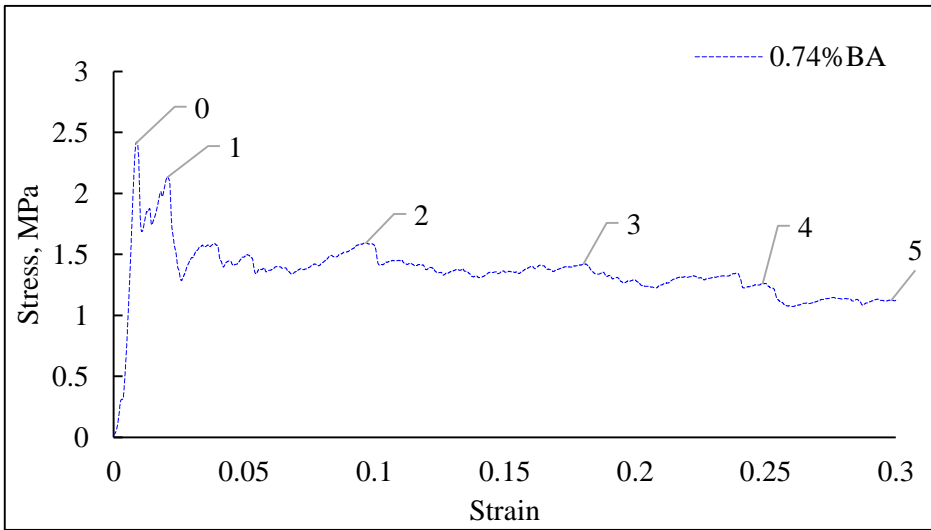
(a)
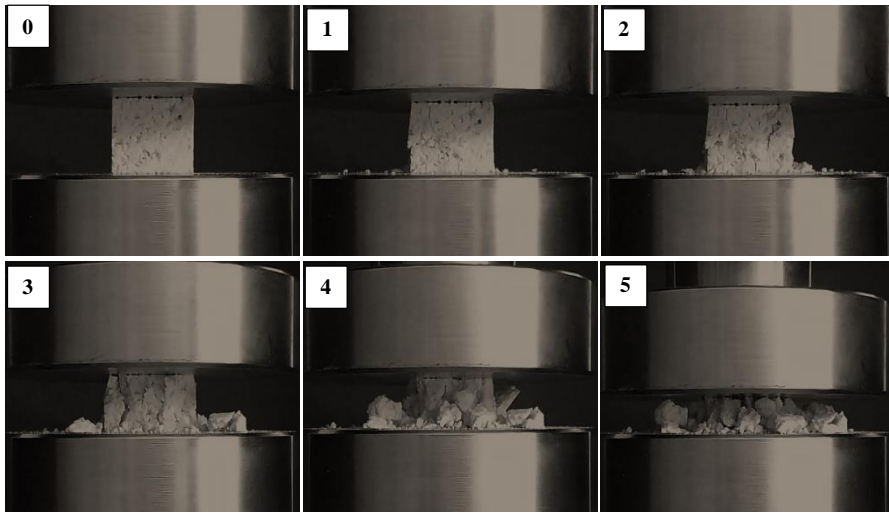
(b)

Fig. 6. (a) A representative stress-strain curve for a specimen with 0.74 wt.% boric acid; and (b) photographs taken during the compression test at various strains.

Effect of Crosshead Speed on the Compressive Properties

Fig. 7 shows the CS of the composites for various boric acid contents at crosshead speeds of 5 mm/min, 100 mm/min, and 400 mm/min. The CS is found to be higher at 100 mm/min crosshead speed irrespective of the boric acid content. The CS at crosshead speed of 400 mm/min appeared to be less than that of 100 mm/min for all boric acid contents. The CS is decreased slightly for samples with boric acid contents of 0.74 wt.%, 2.17 wt.%, and 2.88 wt.%, but it is increased for 0 wt.% and 1.46 wt.% boric acid at crosshead speed 400 mm/min when compared with 5 mm/min. The highest CS is seen in composite with no boric acid for both crosshead speeds (100 mm/min and 400 mm/min) while for a crosshead speed of 5 mm/min the highest CS was seen in composite with 0.74 wt.% boric acid.
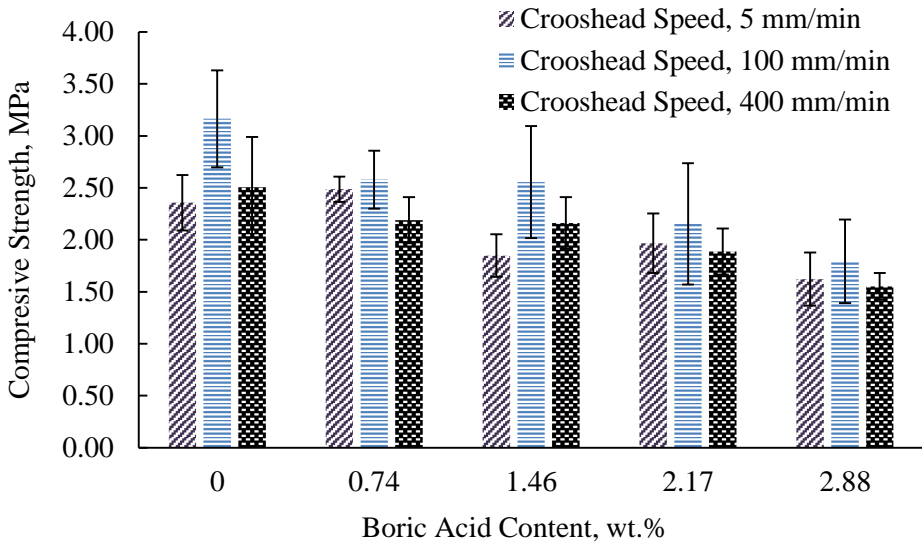
Fig. 7. Compressive strength of composites for various boric acid contents at crosshead speeds of 5 mm/min, 100 mm/min, and 400 mm/min.
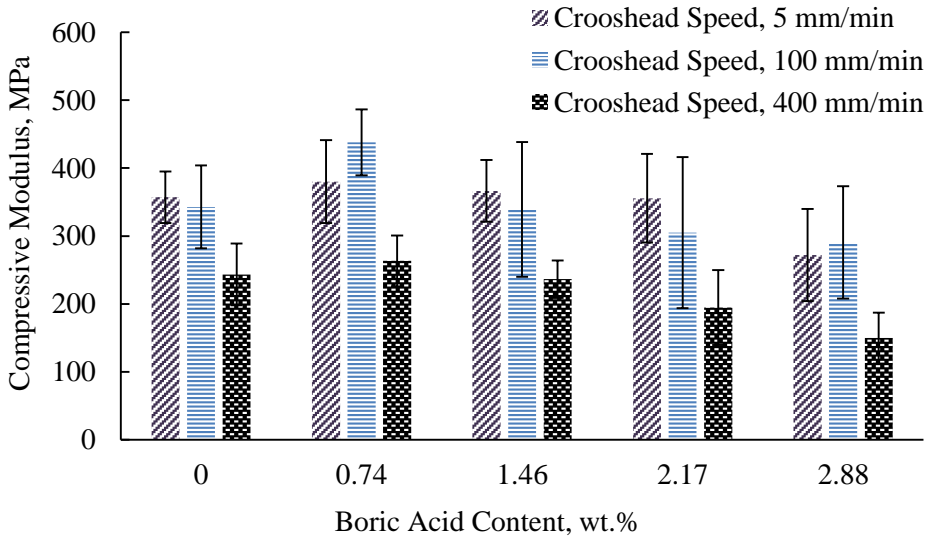

Fig. 8. Compressive modulus for various boric acid contents at crosshead speeds of 5 mm/min, 100 mm/min, and 400 mm/min.

The CM at various crosshead speeds is plotted against different boric acid contents in Fig. 8. The highest value of CM has been found in composites made with 0.74 wt.% boric acid for all three crosshead speeds. Further addition of boric acid in the samples decreased the CM gradually as shown in Fig. 8. A considerable increase in CM (15.21%) is seen in composite with 0.74 wt.% boric acid when the crosshead speed is changed to 100 mm/min from 5 mm/min and the CM is decreased gradually with increasing crosshead speed for all other boric acid contents except the sample with 2.88 wt.% boric acid in which case the CM is slightly higher at a crosshead speed of 100 mm/min.
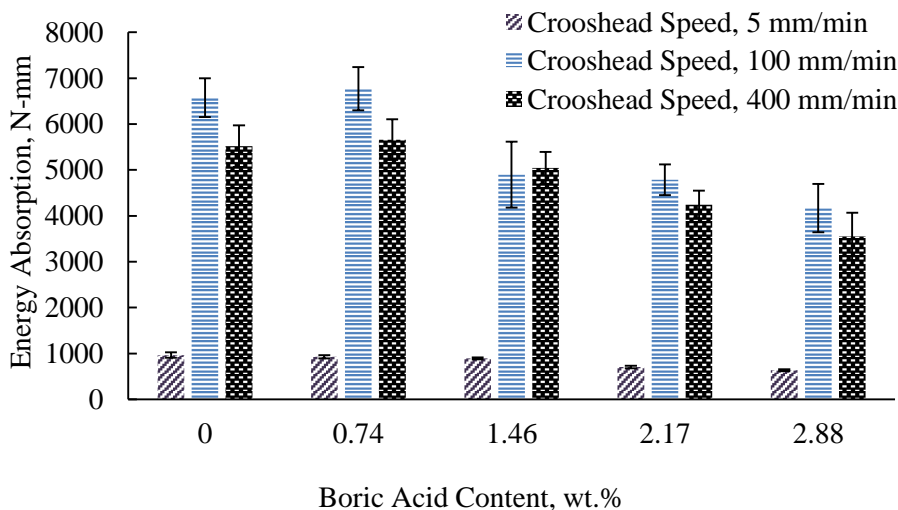

Fig. 9. Total energy absorption up to 50% deformation for various boric acid contents at crosshead speeds of 5 mm/min, 100 mm/min, and 400 mm/min.

In Fig. 9, the total energy absorption up to 50% deformation during compression tests for various boric acid contents and crosshead speeds is given as a bar chart. The highest EA is observed at a crosshead speed of 100 mm/min for specimens with 0 wt.% and 0.74 wt.% boric acid but the EA is decreased at a crosshead speed of 400 mm/min though it is higher than the control sample. In the case of foam with 1.46 wt.% boric acid, EA appeared to be the highest at a crosshead speed of 400 mm/min. However, the EA in the specimens with 2.17 wt.% and 2.88 wt.% boric acid decreased gradually with the increase in crosshead speed. The percent increase in EA is seen to be 17.28% and 11.59% for a sample made of 0 wt.% and 0.74 wt.% boric acid respectively at a crosshead speed of 100 mm/min when compared with 5 mm/min.

Various composite foam materials show strain rate sensitivity as identified by the researchers [30-33]. *Dauod* found that yield strength, plateau stress, and energy absorption increased with increasing strain rate for the glass microballons reinforced Zn12Al foam [30]. *Bouix et al.* investigated polypropylene foam at various strain rates and also reported that plateau stress, yield stress, and plateau stress modulus increased with increasing strain rate [31]. *Woldesenbet et al.* also showed that the peak stress increased with increasing strain rate for their composite foam made of epoxy and microballons [33]. However, *Mondal et al.* found that the plateau stress decreased with increasing strain rate for their closed cell Aluminum-fly ash composite foam [34]. During

the compression test, the strain rate is highly related to the crosshead speed. The approximate strain rate can be calculated by dividing the crosshead speed by the specimen thickness or from the slope of the time versus strain curves. In terms of compressive strength, the composite foams in this work showed that the CS increased when the strain rate increased from 0.004 s^{-1} to 0.08 s^{-1} while it decreased at a strain rate of approximately 0.32 s^{-1} (see Fig. 7). This trend is somewhat different than the observations of Refs. [30, 31, 33] where the researchers have found a continuously increasing trend of CS with the increase in strain rate though they investigated a wide range of strain rates. The compressive modulus appeared to be decreased with increasing strain rate except for the foams with 0.74 wt.% and 2.88 wt.% boric acid (see Fig. 8). This observation is analogous to the finding of *Dauod* for his composite foam made of 30 % glass microballons and Zn12Al foam [30]. The composite foams made with 0 wt.% and 0.74 wt.% boric acid showed a significant increase in EA at higher strain rates (0.08 s^{-1} and 0.32 s^{-1}) compared to the quasi-static strain rate of approximately 0.004 s^{-1} while further addition of boric acid in the composite foam caused a decrease in EA with increasing strain rate (see Fig. 9). However, the energy absorption decreased when the strain rate is increased from 0.08 s^{-1} to 0.32 s^{-1} for all composite foams except the foam with 1.46 wt.% boric acid.

Many researchers have studied the effect of strain rate on compressive properties of foam material made of different materials and found that the compressive strength, modulus, and energy absorption increase with increasing strain rate. However, most of them used a high matrix volume fraction for their foams as well as the studies were also based on very high strain rates. In this work, the expanded perlite is used as a primary filler for manufacturing the foam which has a unique internal cellular structure. Again the matrix volume fraction used in manufacturing perlite foams is also very small compared to the void volume fraction. So, it is not unusual to get different compressive behavior for expanded perlite-based foams at different strain rates. The range of strain rates studied in this work is not suitable to conclude the strain rate effect of perlite-based composites. It may be future work to investigate a larger range of strain rates for a complete understanding of the effects of strain rates on the compressive properties of the expanded perlite-based foams. Nonetheless, the results presented in the paper provide a good indication that the perlite composite foams developed in this work are sensitive to strain rate.

Effect of Crosshead Speed on the Stress-Strain Curves

To show the effect of crosshead speed on the stress-strain curves Fig. 10 is given. In Fig. 10 (a), it can be seen that the trend of stress-strain curves for crosshead speeds of 100 mm/min and 400 mm/min are similar to that of quasi-static crosshead speed of 5 mm/min. The trend is already discussed in section 4.2. However, one significant difference is noticed in the elastic region of the stress-strain curve that is the small plateau region is gradually disappeared in the stress-strain curves when the crosshead speed is increased from 5 mm/min to 100 mm/min to 400 mm/min (see Fig. 10 (b)). It is because the higher speed of testing has eliminated the effect of surface irregularities (see Fig. 5 (c)) due to perlite particles.
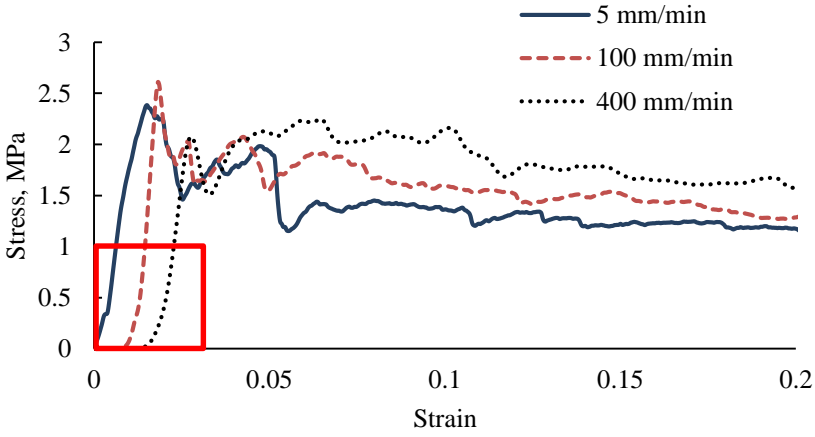
(a)
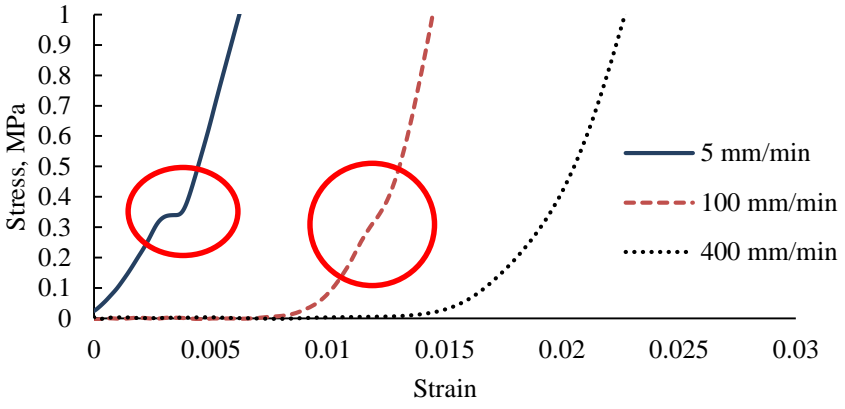
(b)

Fig. 10. (a) Stress-strain curves for specimens with 0.74 wt.% boric acid at crosshead speeds of 5 mm/min, 100 mm/min, 400 mm/min, and (b) magnified curves in Fig. 10 (a), the area marked by the rectangle.

Hygroscopic Behavior

The percentage increase in mass of the composites is plotted for various boric acid contents in Fig. 11 at immersion times of 24 and 48 hours. A maximum increase in mass (103.13% and 106.98%, at 24 and 48 hours, respectively) was seen in the sample having no boric acid and the minimum is seen for 1.46 wt.% boric acid (89.27% and 95.02% at 24 and 48 hours respectively). The mass gain decreased with increasing boric acid content up to 1.46 wt.% and an anomaly is noticed with a further increase in boric acid content in the composite. Expanded perlite particles are highly porous, containing a volume fraction of open pores of approximately 87-90%, according to *Arifuzzaman and Kim* [19]. In addition, the sodium silicate solution after dehydration at low temperature, which is the

current case, and gypsum have a very high affinity to water [35, 36]. Therefore, it is highly likely that the composite foam made of expanded perlite particles, sodium silicate solution, and gypsum to absorb a significant amount of water into the porous structure of the composite. It can be noted that this composite material is not suitable for outdoor application, rather it should be used in drywall conditions. Another benefit of high-water absorption is that these materials are suitable for humidity control in the indoor environment because of their high moisture buffering capacity. Nonetheless, the addition of boric acid in the composite has reduced the water absorption in the composite significantly. The maximum reduction of 13.44% in water absorption is seen on the composite with 1.46 wt.% boric acid at 24 hours of immersion into distilled water. On the other hand, an 11.58% reduction in water absorption is seen for foam made of 2.88 wt.% boric acid at 48 hours of immersion into distilled water. The reduction of water absorption is because boric acid reacts with sodium silicate and the B^{3+} ion replaces the Si^{4+} ion in the SiO_4 structure [25]. Thus the stability of colloidal sodium silicate solution is increased and as a result, when dehydrated the amount of water absorption is reduced.
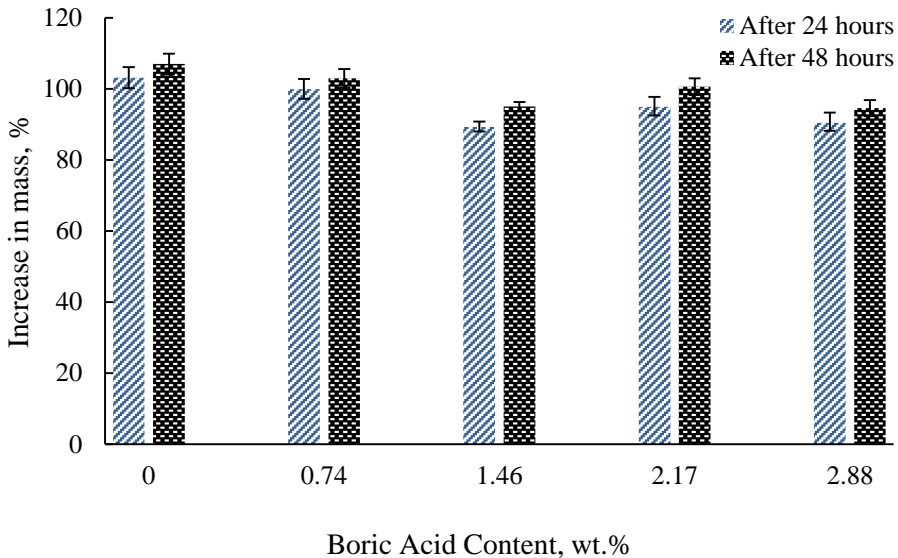

Fig. 11. The percentage increase in mass after 24 and 48 hours of immersion into distilled water for various boric acid contents (Standard deviations are shown as error bars).

<u>Density and Compressive Properties after Hygroscopic Test</u>

Figs. 12 and 13 show the CS and CM of the composites for various boric acid contents before and after 48 hours of immersion into distilled water. It can be observed that the water absorption due to hygroscopic tests affected both the CS and CM significantly. One of the basic reasons for the reduction of strength and modulus is that the dried sodium silicate is dissolved in the water and defused out of the sample. This is supported by the decrease in density of the dried samples given in Table 3. However, the structural integrity of the samples was not affected by the hygroscopic tests. The CS and CM of the wet specimens after the hygroscopic test are seen as higher than the respective

dried ones because of the trapped water into the porous structure of the composites. Both CS and CM appeared to be increased with the addition of up to 1.46 wt.% boric acid, but further addition of boric acid caused a decrease in CS and CM as seen in Figs. 12 and 13.

Table 3. Density of the specimens before and after the hygroscopic test.

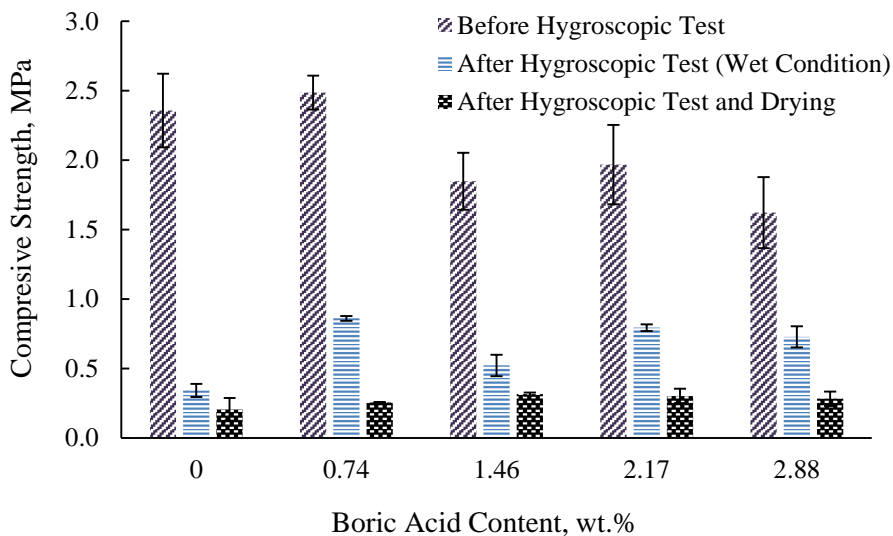| Boric Acid Content, wt.%	Density Before Water Absorption, g/cm^3	Density After Drying, g/cm^3	Percentage Decrease After Drying, %
0	0.407	0.310	61.68
0.74	0.419	0.314	60.78
1.46	0.423	0.333	56.52
2.17	0.426	0.383	52.87
2.88	0.427	0.346	54.88

*Fig. 12. Compressive strength for various boric acid contents
(standard deviations are shown as error bars).*

In Fig. 14, the total energy absorption up to 50% deformation during the compression test for various boric acid contents is plotted from the results of the compression tests before and after the hygroscopic tests. The EA of the fresh specimens for all boric acid content before the hygroscopic test is seen to be the highest and it decreased drastically after the hygroscopic test. The EA of the wet specimens (after 48 hours of immersion in the distilled water) after the hygroscopic test is seen to be higher than the dried specimens after the hygroscopic test because of the water entrapment in the porous foams. It is also observed that the EA of the dried specimens after hygroscopic tests gradually increased with increasing boric acid content in the composite foam. From this analysis, it can again be said that the composites developed here are only suitable for a dry environment and further work is necessary to improve the performance of the composites to be used in a wet environment.
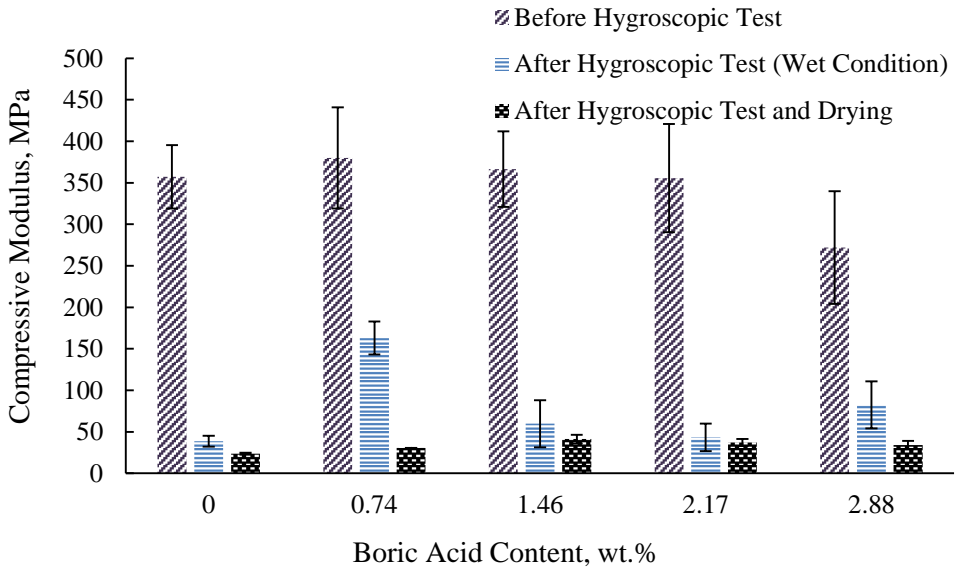
Fig. 13. Compressive modulus for various boric acid contents
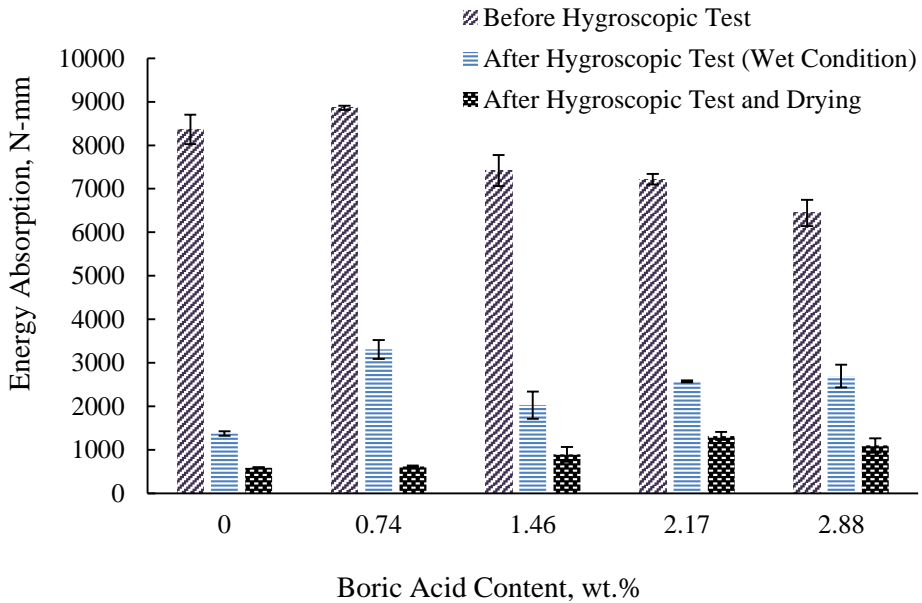*(standard deviations are shown as error bars).*

Fig. 14. Total energy absorption up to 50% deformation for various wt.% of boric acid
(standard deviations are shown as error bars).

Conclusions

Expanded perlite/sodium silicate composite foams were manufactured using various boric acid contents to investigate the effect of boric acid on compressive and hygroscopic behavior. The summary of the outcomes of this work is given below:

- The addition of boric acid in the EP/sodium silicate composite foams increased the density linearly with a high correlation coefficient because of the increased mass due to the addition of boric acid. A maximum increase in density was 4.91 % for a boric acid content of 2.88 wt.% was found.

- The highest compressive strength, compressive modulus, and energy absorption were found in the foam manufactured using 0.74 wt.% boric acid and further addition of boric acid caused a gradual decrease in compressive properties. The building materials discussed in this study displayed the specific compressive strength range of 3.80-5.93 MPa/(g/cm^3) which are well compatible with the lightweight building boards available in the literature in terms of their compressive strength and lightweight.

- The stress-strain curves showed a small plateau in the elastic region because of the irregular specimen surface. The failure of all composite foams was identified to be the multiple cracking/sliding planes mode. A long plateau (up to approximately 50% strain) after failure was noticed in the stress-strain curves for all foams indicating the high energy absorption capability of the composites.

- The developed composite foams appeared to be highly sensitive to the strain rate of the compression test. Among the three strain rates (0.004 s^{-1}, 0.08 s^{-1}, 0.32 s^{-1}) considered in this study, the compressive strength was found to be the highest at the strain rate of 0.08 s^{-1} for all foams. The compressive modulus showed a decreasing trend with increasing strain rate except for the foam with 0.74 wt.% boric acid. The energy absorption was the highest for the control foam and the foam with 0.74 wt.% boric acid and it decreased with increasing strain rate for the foams with 1.46 % and 2.88 % boric acid by weight.

- The plateau in the elastic region of the stress-strain curves gradually disappeared with increasing strain rate because of the high crosshead speed which eliminated the effect of surface irregularities.

- The water absorption decreased with increasing boric acid content in the foam and a maximum reduction of 13.44 % was seen on the foams manufactured with 1.46 wt.% boric acid after 24 hours of immersion into distilled water. After 48 hours of immersion, the maximum reduction (11.59%) in water absorption is seen in the foam made of 2.88 wt.% boric acid. The reduction in water absorption is due to the chemical reaction between sodium silicate solution and boric acid.

- Although the water absorption was reduced and compressive properties after hygroscopic tests were improved with the addition of boric acid, the composites are not recommended for a wet environment because of the considerable decrease in compressive properties after hygroscopic tests when compared with specimens before the hygroscopic test.

Acknowledgments

References

[1]   A.M. Rashad: Constr Build Mater, 121 (2016) 338-353.
[2]   O.A. Qasim: Int J Civ Eng, 9 (2018) 371-387.
[3]   J. Y. Xue Zhang: Appl Mech Mater, 584 (2014) 1835-1838.
[4]   O. Sengul, et al.: Energy Build, 43 (2011) 671-676.
[5]   P. Pramusanto, et al.: IOP Conf. Ser.: Mater Sci Eng, 830 (2020) 042040.
[6]   S. Celik, R. Family, M.P. Menguc: J Build Eng, 6 (2016) 105-111.
[7]   R. Ye, et al.: Materials, 8 (2015) 7702-7713.
[8]   T.S. Bozkurt, S.Y. Demirkale: Acoust Aust, 48 (2020) 375–393.
[9]   X. Yanjun, et al.: Open Mater Sci, 9 (2015) 39-42.
[10]   C. Yao, et al.: Energy Convers Manag, 155 (2018) 20-31.
[11]   D. Sun, L. Wang: Constr Build Mater, 101 (2015) 791-796.
[12]   G. Jia, et al.: J. Non-Cryst Solids, 482 (2018) 192-202.
[13]   X.W. Wu, et al.: Environ Prog Sustain Energy, 37 (2018) 1319-1326.
[14]   L. Fu, t al.: Renew Energy, 114 (2017) 733-743.
[15]   Alam, M., et al.: Energy Build, 69 (2014) 442-450.
[16]   H. Gao, et al.: Energy Build, 200 (2019) 21-30.
[17]   Y. Lin, X. Li, Q. Huang: Energy Build, 231 (2021) 110637.
[18]   B. Skubic, M. Lakner, I. Plazl: Ind Eng Chem Res, 52 (2013) 10244-10249.
[19]   M. Arifuzzaman, H.S. Kim: Constr Build Mater, 93 (2015) 230-240.
[20]   P. Adhikary, M. Arifuzzaman, E. Kabir: J Eng Adv, 1 (2020) 1-5.
[21]   Y.L. Tian, et al.: Appl Mech Mater, 405-408 (2013) 2771-2777.
[22]   Ü. Ağbulut: J Therm Eng, 4 (2018) 2274-2286.
[23]   H. Gao, et al.: Energy Build, 190 (2019) 25-33.
[24]   J. Zhang, et al.: Energy Build, 92 (2015) 155-160.
[25]   Y. Li, et al.: J Alloys Compd, 666 (2016) 513-519.
[26]   D. Shastri, H.S. Kim: Constr Build Mater, 60 (2014) 1-7.
[27]   A. Çolak: Cem Concr Compos, 22 (2000) 193-200.
[28]   A. Vimmrová, et al.: Cem Concr Compos, 33 (2011) 84-89.
[29]   H. Allameh-Haery, E. Kisi, T. Fiedler: J Cell Plast, 53 (2016) 425-442.
[30]   A. Daoud: Mater Sci Eng A, 525 (2009) 7-17.
[31]   R. Bouix, P. Viot, J.-L. Lataillade: Int J Impact Eng, 36 (2009) 329-342.
[32]   M.D. Goel, et al.: Materials Science and Engineering: A, 590 (2014) 406-415.
[33]   E. Woldesenbet, N. Gupta, A. Jadhav: J Mater Sci, 40 (2005) 4009-4017.
[34]   D.P. Mondal, M.D. Goel, S. Das: Mater Des, 30 (2009) 1268-1274.
[35]   Y.A. Owusu: Adv Colloid Interface Sci, 18 (1982) 57-91.
[36]   A. Bicer, F. Kar: Therm Sci Eng Prog, 1 (2017) 59-65.